Optical recombination from excited states in Ge/Si self-assembled quantum dots

P. Boucaud,* S. Sauvage, M. Elkurdi, E. Mercier, T. Brunhes, V. Le Thanh, and D. Bouchier
Institut d'Électronique Fondamentale, UMR CNRS 8622, Bâtiment 220, Université Paris-Sud, 91405 Orsay, France

O. Kermarrec, Y. Campidelli, and D. Bensahel
STMicroelectronics 850 Rue Jean Monnet, 38926 Crolles Cedex, France

(Received 6 February 2001; revised manuscript received 9 April 2001; published 18 September 2001)

We have investigated the photoluminescence of single and multiple layers of Ge/Si self-assembled quantum dots as a function of the excitation power density. We show that the photoluminescence of the quantum dots is strongly dependent on the pump excitation power. The photoluminescence broadens and is blueshifted by as much as 80 meV as the power excitation density increases. Meanwhile, the photoluminescence associated with the two-dimensional wetting layers exhibits only a weak dependence on the pump excitation power. This significant blueshift is interpreted in terms of state filling and recombination from the confined excited hole states in the dots. The photoluminescence data are correlated to the density of states as calculated by solving the three-dimensional Schrödinger equation in these islands with a lateral size of the order of 100 nm.

DOI: 10.1103/PhysRevB.64.155310 PACS number(s): 78.67.Hc, 78.55.−m, 73.21.La, 71.20.Nr

I. INTRODUCTION

The recombination processes in SiGe/Si heterostructures have been extensively studied in recent years. The radiative band-edge recombination of free and bound excitons associated with shallow impurities have been evidenced in bulk or strained SiGe/Si quantum well samples.[1] Localized excitons bound to a strain field created by Ge platelets were observed in samples grown by molecular beam epitaxy.[2] At low excitation density, excitons localized by regions with higher Ge content than the average alloy content were observed in SiGe/Si quantum wells.[3] A broad recombination band associated with isoelectronically trapped excitons was also reported.[4] The statistical properties of the alloys were often cited as an intrinsic source of broadening and localization.[5]

Since the direct observation of the formation of Ge/Si self-assembled quantum dots by a Stranski-Krastanow growth mode,[6] a considerable interest is devoted to the properties of these islands grown on Si. By depositing Ge either by molecular-beam epitaxy or by chemical vapor deposition, the spontaneous nucleation of Ge/Si islands is observed beyond a critical thickness of four Ge monolayers. The photoluminescence which is a sound spectroscopic tool for the study of the islands has been reported by several groups. A broad recombination band associated with the interband photoluminescence of the islands is usually observed.[7] The radiative recombination of the carriers localized in the two-dimensional wetting layers is also usually observed. The Ge/Si self-assembled islands exhibit a small aspect ratio (height/base). The typical height of capped quantum dots is around a few nm while the lateral size of the islands remains large, of the order of 100 nm.[8,9] One does not expect a strong lateral confinement for this range of in-plane sizes. As opposed to standard InAs/GaAs self-assembled islands which exhibit a strong three-dimensional confinement, the confinement in Ge/Si islands is expected to be strong in the growth direction but weak in the layer plane. However, the in-plane heavy hole effective mass in tetragonally strained GeSi alloys is weak. The density of states in Ge/Si islands is therefore intermediate between the density of states of a strongly confined system and the density of states of a two-dimensional layer. A signature of this feature should be observed in the photoluminescence recombination spectra of the islands.

In this work, we have investigated the photoluminescence properties of Ge/Si self-assembled islands grown by chemical vapor deposition. The photoluminescence is studied as a function of the excitation power density. The power density is scanned over five orders of magnitude from 20 μW to 2.5 W. Whereas the photoluminescence of the two-dimensional wetting layers is weakly dependent on the excitation density, the photoluminescence of the islands exhibit a very strong dependence on the illumination power. The photoluminescence broadens and shifts to higher energy by about 80 meV as the excitation density increases. This behavior indicates that the quantum dot ground-state recombination is only observed at low excitation power and that at high excitation power the recombination from the excited states are dominating the photoluminescence, while the ground-state recombination is still present. At high excitation power densities, the radiative recombination associated with the excited hole states is characterized by a broad asymmetric line shape with a long tail towards low energy. Phonon-assisted recombinations contribute to the broadening of the photoluminescence at low energy. The strong photoluminescence shift, which is much larger than the one expected from band bending effects, indicates that the effect of state filling is significant in these islands. This blueshift is correlated to the density of states in the islands calculated by solving the three-dimensional Schrödinger equation for the heavy holes. We emphasize that the observation of the photoluminescence of the excited states is obtained for a moderate excitation power because of the long recombination times in these indirect band-gap semiconductors, i.e., the photoexcited carrier density is much larger for a given pump intensity than the one measured in III-V materials. These results also demonstrate that the excitation density should be carefully taken into ac-

count in order to compare photoluminescence results from samples to samples.

The investigated samples were grown on Si(001) by chemical vapor deposition either at low or high pressure. Silane and germane diluted in hydrogen carrier gas were used as gas precursors. For the samples deposited at low pressure, the growth temperature was 600 °C and the gas pressure around 5×10^{-4} Torr during epitaxial growth. For the samples deposited at high pressure in an industrial lamp-heated single wafer chemical vapor deposition reactor,[10] the growth temperature was 625 °C, at a total pressure lower than 100 Torr. Two types of samples were studied: (i) a single layer of buried Ge/Si self-assembled quantum dots, and (ii) a multiple stacking of ten Ge/Si self-assembled quantum dot layers separated by 30-nm barriers with a good uniformity from layer to layer. This uniformity was achieved by adjusting the amount of deposited Ge from layer to layer to compensate the decrease of the critical thickness induced by strain field of buried islands.[11] The achievement of uniform multiple layers ensures that the photoluminescence data are not dependent on the vertical stacking of the layers. The quantum dots were characterized by cross-section transmission electron microscopy. The typical height of the quantum dot is around 6 nm and the lateral size is around 100 nm. The dot density of the samples grown at low (high) pressure is around 2 $(6)\times10^{9}\,\mathrm{cm}^{-2}$.[11] The dots have a lens or dome shape geometry with a circular base. It is well known that the embedding of the nanoscale islands can change the composition and the shape of the dots.[12] The driving mechanism for the formation of the islands is the strain relaxation. This strain relaxation can be assisted by a strong intermixing, i.e., the incorporation of Si into the islands.[13] Selective area electron diffraction pattern have shown that the average composition of buried Ge/Si self-assembled islands grown by chemical vapor deposition is around 50%.[14] These measurements did also indicate that a small composition gradient was present within the islands.

The photoluminescence of the samples mounted in an helium-cooled cryostat was excited nonresonantly with the 488-nm line of an argon ion laser. The photoluminescence was dispersed by a 0.64-m monochromator and detected with a liquid-nitrogen-cooled Ge photodiode using standard lock-in techniques. The photoluminescence data were not corrected for the spectral sensitivity of the detector but we have separately checked with an InAs photodetector that the photoluminescence spectrum was not significantly modified by the Ge detector cutoff energy.

II. PHOTOLUMINESCENCE RESULTS

Figure 1(a) shows the low-temperature photoluminescence of a multiple layer of uniform Ge/Si self-assembled quantum dots as a function of the excitation power density. The photoluminescence of the quantum dots is observed to the low-energy side of the spectrum around 800 meV. At energies above 900 meV, the recombination is associated with the no-phonon (NP) and phonon-assisted (TO) radiative recombination in the wetting layers. Two groups of lines separated by the Si-Si optical phonon energy can be distinguished in the wetting layer recombination.[15] In Fig. 1(a), the excitation power density varies over five orders of magnitude. The photoluminescence amplitude has been normalized to the photoluminescence of the self-assembled quantum dots. The quantum dot luminescence is dominated by a no-phonon recombination line. A small shoulder as shown for example on the curve corresponding to a $0.2\text{-mW}\,\mathrm{cm}^{-2}$ excitation intensity can be observed at lower energy. This shoulder corresponds to a phonon-assisted recombination. The energy difference between these two resonances is close to 36 meV, a value which corresponds to Ge-Ge phonon energies. The broadening of the photoluminescence is only 35 meV at low excitation density. This value represents the inhomogeneous broadening of the photoluminescence associated with the size and composition fluctuations of the dots.

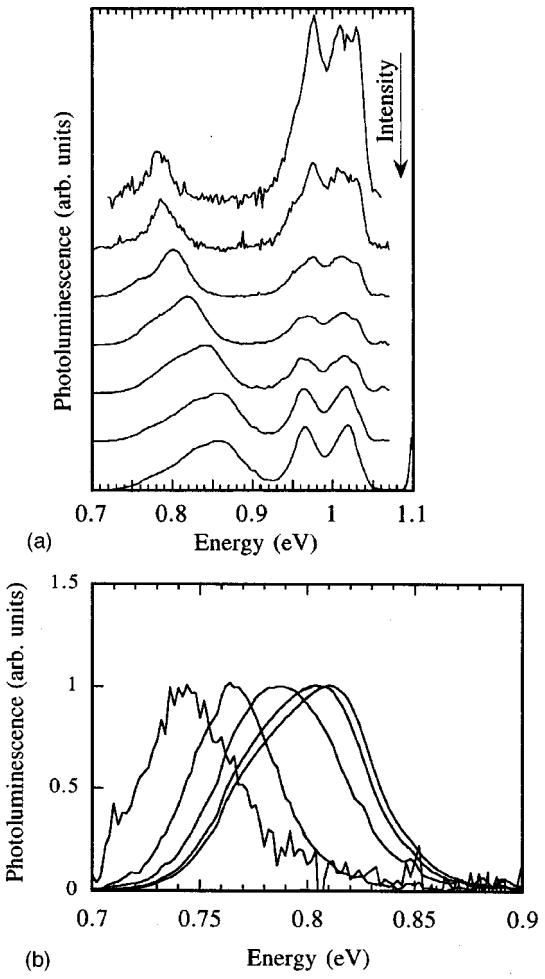

FIG. 1. (a) Low-temperature (5 K) photoluminescence of a multiple layer of uniform Ge/Si quantum dots as a function of the excitation power density. The power density is, from top to bottom, 2×10^{-4}, 4×10^{-4}, 4×10^{-3}, 4×10^{-2}, 4×10^{-1}, 4, and 10 $\mathrm{W\,cm}^{-2}$. The amplitude of the quantum dot photoluminescence has been normalized to unity. The curves are offset for clarity. (b) Low-temperature (5 K) photoluminescence of a single layer of Ge/Si quantum dots as a function of the excitation power density. From left to right, the excitation power density is 4×10^{-3}, 4×10^{-2}, 4×10^{-1}, 2, and $4\ \mathrm{W\,cm}^{-2}$. The amplitude of the quantum dot photoluminescence has been normalized to unity.

We emphasize that a broadening of 35 meV is significantly smaller than the one previously reported.[11,15] The striking feature reported in Fig. 1(a) is the strong dependence of the peak energy and of the broadening of the quantum dot photoluminescence as a function of the excitation power density. A blueshift of the photoluminescence peak as large as 80 meV is observed between the low and the high excitation power density spectra. For the same excitation conditions, the photoluminescence associated with the two-dimensional wetting layer exhibits a much smaller change. For the wetting layers, the major difference observed as the excitation power density increases is a progressive change in the transitions which dominate the recombination spectrum. This behavior has to be compared with the one reported for SiGe quantum wells vs excitation power density that was extensively studied in past years. The photoluminescence shifts observed in these cases were much smaller, up to 20 meV. The influence of band bending effects and of the staggered band lineup between Si and strained SiGe was mentioned to explain the photoluminescence shifts.[16,17] A similar shift, associated with the increase of the quantization energy of electrons localized at the interface, was also reported in a type-II heterosystem formed by GaSb/GaAs quantum dots.[18] It is clear that the shifts observed with the Ge quantum dot luminescence are more important than those observed with quantum wells. Moreover, a significant broadening of the emission is simultaneously observed with the spectral shift, thus ruling out the space-charge effects associated with band bending as the dominant mechanisms. Figure 1(b) shows the photoluminescence of a single layer of Ge/Si quantum dots for different excitation power densities, thus illustrating that the same effect is observed for a single layer of Ge/Si dots.

Figure 2(a) shows the photoluminescence peak energy shift and the broadening (b) as a function of the pump excitation density. Figure 2(c) shows the integrated intensity of the quantum dot photoluminescence. Three regions can be distinguished in Figs. 2(a) and (b). At low excitation power density, the photoluminescence peak energy and the broadening are constant. We only observe an increase of the photoluminescence amplitude with the excitation density. Above 4 $\mathrm{mW\,cm^{-2}}$, the photoluminescence peak energy increases with a slope of around 20 meV/decade. The broadening of the photoluminescence increases meanwhile significantly. Above 4 $\mathrm{W\,cm^{-2}}$, the peak energy and the broadening remain constant. The amplitude of the quantum dot photoluminescence continue to increase but less significantly than for the wetting layers. For this excitation density range, the photoluminescence of the wetting layers is characteristic of the photoluminescence of a confined electron-hole plasma.[19] We emphasize that similar photoluminescence spectra were obtained for *single* quantum dot layers grown with a high pressure chemical vapor deposition reactor. These data are therefore characteristic of these Ge/Si self-assembled quantum dots. Regarding the integrated intensity, there is a balance between the wetting layer photoluminescence and the quantum dot photoluminescence at low excitation density. Above 2 $\mathrm{mW\,cm^{-2}}$, the integrated luminescence exhibits a sublinear behavior as a function of the pump excitation density. This sublinear behavior is most likely associated with the increasing probability of nonradiative Auger-assisted relaxation mechanisms.[20]

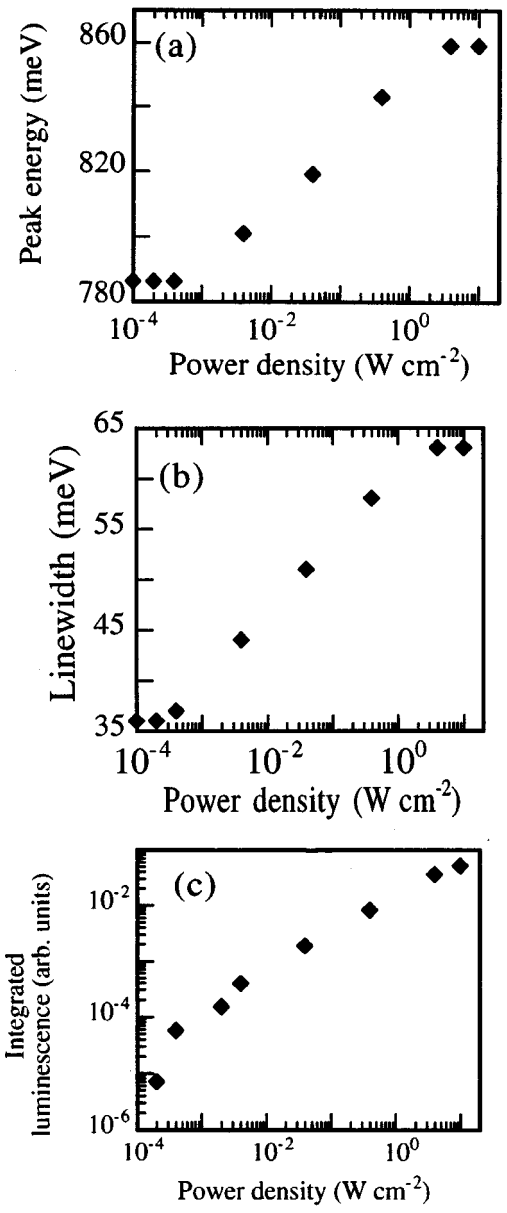

FIG. 2. (a) Photoluminescence peak energy as a function of the excitation power density. Figure (b) shows the broadening of the photoluminescence. Figure 2(c) shows the integrated quantum dot photoluminescence as a function of the excitation power density.

An upper limit of the photoinduced sheet carrier density n_{2D} can be estimated from the pump excitation density (1):

$$n_{2D} = I\tau/h\nu, \tag{1}$$

where I is the pump excitation intensity, τ the carrier lifetime, and $h\nu$ the excitation energy. Assuming a typical recombination time of 1 μs in this indirect band-gap material,[21] one expects a maximum sheet carrier density of 1×10^{9} $\mathrm{cm^{-2}}$ for a 0.4-$\mathrm{mW\,cm^{-2}}$ intensity. The decay time of 1 μs is only given as an indication. It could be even higher at low excitation densities where the nonradiative Auger re-

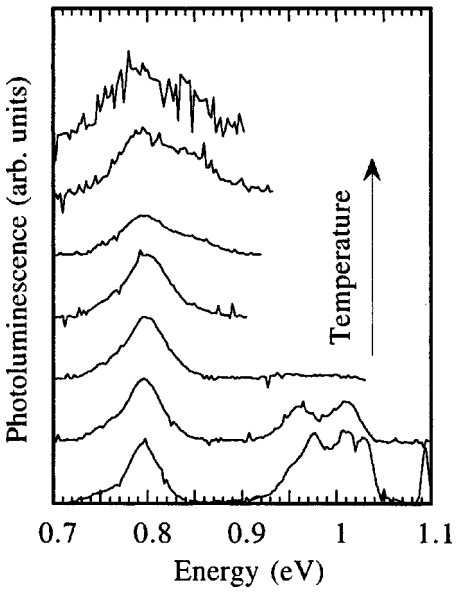

FIG. 3. Temperature dependence of the quantum dot photoluminescence. From bottom to top: 4, 10, 50, 100, 150, 200, and 250 K. The excitation power density is 2 mW cm^{-2}. The curves have been offset for clarity. The amplitude of the quantum dot luminescence has been normalized to 1.

combination processes are quenched.[3] This density of 10^9 carriers per square centimeter roughly corresponds to a density of one carrier populating each dot. The onset of the photoluminescence shift and broadening therefore corresponds to the filling of the dot ground state. The broadening of the photoluminescence is thus attributed to the state filling of the quantum dots and to the recombination from the excited states. The increase of broadening is similar to the one observed for example in InAs/GaAs self-assembled quantum dots where the recombination involving excited levels is observed at high excitation densities.[22] We note that while the photoluminescence peak energy and broadening saturate above 4 W cm^{-2}, the amplitude of the photoluminescence still increases above this intensity. We partly attribute this feature to a change of the oscillator strength of the radiative transitions as more carriers are added in the dots and its surrounding. This enhanced oscillator strength could result from a better overlap of the electron and the hole wavefunctions because of additional band bending effects.

Figure 3 shows the dependence of the quantum dot photoluminescence as a function of the temperature. The measurement was performed with a low excitation power density (2×10^{-3} W cm^{-2}). The amplitude of the quantum dot luminescence has been normalized for clarity. While the peak energy of the photoluminescence remains roughly constant over the investigated temperature range, we observe the onset of the photoluminescence broadening above 150 K. At this temperature, a shoulder is observed around 850 meV. This 850-meV energy corresponds to the photoluminescence energy resonance at high excitation power density (see Fig. 1). This feature indicates that in this case the thermal energy is sufficient to populate the excited levels of the dots.

III. DISCUSSION

The photoluminescence results can be analyzed by considering the density of states of the islands. A first step to estimate the density of states would be to consider the very large diameter of the flat dots and to approximate them by a quantum well. The density of states of a two-dimensional hole gas is

$$\frac{dn}{dE}=\frac{m_{\parallel}^{*}}{\pi\hbar^{2}}, \tag{2}$$

where $m_{\parallel}^{*}$ is the in-plane effective mass. dn/dE represents the number of states (dn) per unit area lying in an energy interval dE. In the case of a $Si_{0.5}Ge_{0.5}$ quantum well with $m_{\parallel}^{*}=0.136$ the two-dimensional density of states is 5.7×10^{10} cm^{-2} meV^{-1}. Considering a circular surface with a diameter of 100 nm, i.e., close to the dot base area, this density of states corresponds to 4.5 states per meV, which is equivalent to an average energy spacing of 0.22 meV between the states. Another way to estimate the density of states is to consider a parallelepipedal quantum dot with infinite barrier potentials and a base length of 100 nm. In the latter case, the estimated energy spacing between the first confined levels is around 1 meV. This is much larger than the quantum well approach and suggests that a more accurate calculation is necessary. In order to estimate this density, we have therefore performed single band three-dimensional calculation of the heavy hole energy levels in a quantum dot taking into account a lens-shaped geometry and the finite height of the barrier potential.[23] The calculations were performed with a quantum dot exhibiting an homogeneous core composition of 50% Ge, as observed by electronic diffraction,[14] surrounded by silicon. The height of the lens-shaped dots is 6 nm. The diameter at the base of the dot is 100 nm. The valence band offsets of 350 meV were taken assuming tetragonally strained SiGe on Si.[24] The in-plane heavy hole effective mass was taken as a linear interpolation between the mass of Si ($0.22m_0$) and Ge ($0.058m_0$).[25] The same procedure was used for the effective mass along the z growth axis, $0.206m_0$ in Ge and $0.29m_0$ in Si. We emphasize that this single band calculation is only intended to explain qualitatively the experimental features. A more detailed description of the valence states should be obtained in the framework of a multiband $\mathbf{k}\cdot\mathbf{p}$ calculation. The effective-mass Schrödinger equation is numerically solved using a finite-difference scheme applied on a uniform cell grid of $129\times129\times65$ vertices. The wave functions are set to zero at the edges of the grid, $120\times120\times12$ nm^3 in size. The resulting Hamiltonian matrix is partially diagonalized using an iterative Jacobi-Davidson algorithm.[26] The first 140 energies and wave functions, without spin degeneracy, are calculated in order to get the confined states from the bottom of the confining potential to around 140 meV above the 50% Ge band edge. The potential profile is depicted in the inset of Fig. 4. The calculation did not take advantage of the cylindrical symmetry present in the potential.

Figure 4 shows the calculated density of states for the heavy holes as a function of the energy. Each state is repre-

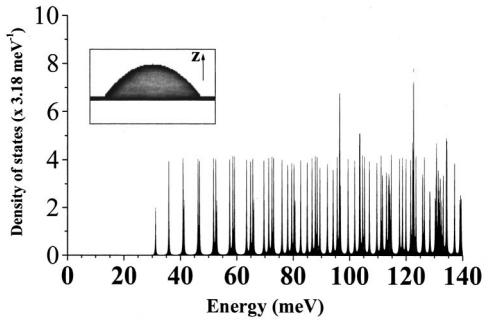

FIG. 4. Density of states for the heavy hole in a lens-shaped Ge/Si quantum dot as a function of the confinement energy. The composition of the quantum dot is 50%. Each state is represented by a Lorentzian with a half width at half maximum of 100 μeV. Inset: potential profile cross section used in the calculation. The dark surface corresponds to a constant vanishing potential. White surface stands for 350 meV. z is the growth axis. The vertical scale is dilated by a factor of 10.

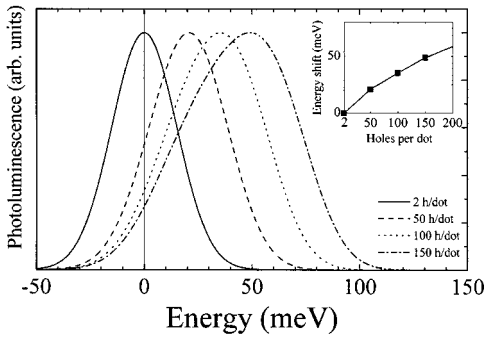

FIG. 5. Calculated photoluminescence spectrum as a function of the number of carriers populating the dots. The inhomogeneous broadening associated with the dot size distribution is taken into account by a Gaussian with a half width σ at $1/\sqrt{e}$ equal to 15 meV. The amplitude of the photoluminescence is normalized to unity. From left to right: 2–5–100–150 carriers per dot. The inset shows the resonance energy shift of the photoluminescence as a function of the number of carriers in the dot. The full line is a guide to the eye.

sented by a Lorentzian with a half width at half maximum of 100 μeV. The amplitude of the density of states, which depends on this homogeneous broadening, is expressed as a function of the number of carriers populating one state, accounting for the spin degeneracy. The energy spacing between the first confined states is around 5 meV, i.e., five times larger than the one roughly estimated with a parallelepipedal quantum dot with infinite barriers and 20 times larger than the one roughly deduced from a quantum well calculation. This difference shows the importance to take into account the geometry and the effective barrier potential. As the confinement energy increases, the energy spacing between the confined levels decreases significantly. Two regions can be clearly distinguished in the distribution of states: first the number of confined states increases slowly as the confinement energy in the dots increases. Around an energy of 60–80 meV above the ground state, the number of confined states for a given energy spacing (i.e., the density of states) increases significantly since these states are closer in energy. The first excited state in the z direction (h_{001}) is calculated at 82 meV above the ground state. This confined state is the first state of a series associated with the onset of a new quasisubband. Without accounting for the spin degeneracy, there are about 90 levels confined in the dots at energies below the energy of this excited state. We note that the light hole states are not considered in this calculation. A rough estimation considering a quantum well with a thickness of 6 nm indicates that these light hole levels should appear around 75 meV above the heavy hole ground state. These states are expected to further increase the density as they appear in the energy spectrum. Considering the number of confined states, we conclude that the density of states in the islands only differ by a factor of 2 as compared to the quantum well case if we consider the levels at an energy higher than 80 meV above the ground state. This feature indicates that in the limit of high energies, the density of states per unit area in the islands tends to the density of states of a two-dimensional layer. It is a direct consequence of the large dot size of the islands. Meanwhile, at energies just above the ground state, the density of states in the islands is significantly lower as compared to the quantum well case.

The calculation of the density of states explains qualitatively the photoluminescence results. Figure 5 shows the line-shape dependence of the photoluminescence as a function of the number of carriers populating the dots. The inhomogeneous broadening associated with the dot size distribution is accounted for by a Gaussian distribution with a half width σ at $1/\sqrt{e}$ equal to 15 meV. The origin of the energy corresponds to the resonance of the photoluminescence in the weak excitation regime. In this calculation based on the density of states shown in Fig. 4, a constant oscillator strength is assumed for each transition. As seen, the filling of the confined hole states leads to a significant blueshift and a significant broadening of the photoluminescence. The asymmetric line shape of the photoluminescence at high carrier densities is well reproduced by the calculation. The significant energy-level separation ($\sim$5 meV) between the first confined states leads first to a large spectral shift. As more carriers are added into the dots, the variation of the photoluminescence is less pronounced. The filling of the dots with 180 carriers (90×2 accounting for the spin degeneracy) leads to a photoluminescence shift of around 60 meV. This filling would correspond to a sheet carrier density of $4\times10^{11}\,\mathrm{cm}^{-2}$. As the dots become more populated, the photoluminescence shift is expected to be reduced since the density of states becomes larger. Populating the dots with more carriers is also more difficult because of the efficiency of the Auger recombination at high carrier densities.[27] At high carrier densities, one expects the wetting layer and the quantum dots to exhibit a similar behavior, i.e., no significant photoluminescence shift, because the density of states in these large islands is not significantly different from that of a two-dimensional layer. We emphasize that we did not consider in this calculation the influence of Coulomb charging for these large dots (100 nm diameter) and the many particle effects.

IV. CONCLUSION

In conclusion, we have shown that the photoluminescence of Ge/Si self-assembled quantum dots is strongly dependent on the power excitation density. The strong photoluminescence blueshift, which is not observed with two-dimensional layers like the wetting layers, has been correlated to the radiative recombination involving excited states of the dots. The density of states in the lens-shaped Ge/Si quantum dots was calculated in order to explain this feature.

ACKNOWLEDGMENT

We acknowledge financial support from Réseaux Micro et NanoTechnologies under Contract No. 00V0091.

*Email address: phill@ief.u-psud.fr

[1] J. C. Sturm, H. Manoharan, L. C. Lenchyshyn, M. L. W. Thewalt, N. L. Rowell, J. P. Noël, and D. C. Houghton, Phys. Rev. Lett. **66**, 1362 (1991).

[2] J. P. Noël, N. L. Rowell, D. C. Houghton, A. Wang, and D. D. Perovic, Appl. Phys. Lett. **61**, 690 (1992).

[3] L. C. Lenchyshyn, M. L. W. Thewalt, J. C. Sturm, P. V. Schwartz, E. J. Prinz, N. L. Rowell, J. P. Noël, and D. C. Houghton, Appl. Phys. Lett. **60**, 3174 (1992); L. C. Lenchyshyn, M. L. W. Thewalt, D. C. Houghton, J. P. Noël, N. L. Rowell, J. C. Sturm, and X. Xiao, Phys. Rev. B **47**, 16 655 (1993).

[4] A. Hartmann, L. Vescan, C. Dieker, T. Stoica, and H. Lüth, Phys. Rev. B **48**, 18 276 (1993).

[5] A. Fried, A. Ron, and E. Cohen, Phys. Rev. B **39**, 5913 (1989).

[6] D. J. Eaglesham and M. Cerullo, Phys. Rev. Lett. **64**, 1943 (1990).

[7] P. Schittenhelm, M. Gail, J. Brunner, J. F. Nützel, and G. Abstreiter, Appl. Phys. Lett. **67**, 1292 (1995); H. Sunamura, N. Usami, Y. Shiraki, and S. Fukatsu, *ibid.* **66**, 3024 (1995); O. G. Schmidt, C. Lange, and K. Eberl, *ibid.* **75**, 1905 (1999); V. Le Thanh, P. Boucaud, D. Débarre, D. Bouchier, and J. M. Lourtioz, Phys. Rev. B **58**, 13 115 (1998).

[8] Y. W. Mo, D. E. Savage, B. S. Swartzentruber, and M. G. Lagally, Phys. Rev. Lett. **65**, 1020 (1990).

[9] G. Abstreiter, P. Schittenhelm, C. Engel, E. Silveira, A. Zrenner, D. Meertens, and W. Jäger, Semicond. Sci. Technol. **11**, 1521 (1998).

[10] C. Hernandez, Y. Campidelli, D. Simon, D. Bensahel, I. Sagnes, G. Patriarche, P. Boucaud, and S. Sauvage, J. Appl. Phys. **86**, 1145 (1999).

[11] V. Le Thanh, V. Yam, P. Boucaud, F. Fortuna, C. Ulysse, L. Vervoort, D. Bouchier, and J.-M. Lourtioz, Phys. Rev. B **60**, 5851 (1999).

[12] P. Sutter and M. G. Lagally, Phys. Rev. Lett. **81**, 3471 (1998).

[13] S. A. Chaparro, J. Drucker, Y. Zhang, D. Chandrasekahr, M. R. McCartney, and D. J. Smith, Phys. Rev. Lett. **83**, 1199 (1999).

[14] G. Patriarche, I. Sagnes, P. Boucaud, V. Le Thanh, D. Bouchier, C. Hernandez, Y. Campidelli, and D. Bensahel, Appl. Phys. Lett. **77**, 370 (2000).

[15] V. Yam, Vinh Le Thanh, Y. Zheng, P. Boucaud, and D. Bouchier, Phys. Rev. B **63**, 033 313 (2001).

[16] T. Baier, U. Mantz, K. Thonke, R. Sauer, F. Schäffler, and H. J. Herzog, Phys. Rev. B **50**, 15 191 (1994).

[17] M. L. W. Thewalt, D. A. Harrison, C. F. Reinhart, J. A. Wolk, and H. Lafontaine, Phys. Rev. Lett. **79**, 269 (1997).

[18] F. Hatami, N. N. Ledentsov, M. Grundmann, J. Böhrer, F. Heinrichsdorff, M. Beer, D. Bimberg, S. S. Ruvimov, P. Werner, U. Gösele, J. Heydenreich, U. Richter, S. V. Ivanov, B. Ya Meltser, P. S. Kop'ev, and Zh. I. Alferov, Appl. Phys. Lett. **67**, 656 (1995).

[19] X. Xiao, C. W. Liu, and J. C. Sturm, Appl. Phys. Lett. **60**, 1720 (1992).

[20] R. Apetz, L. Vescan, A. Hartmann, C. Dieker, and H. Lüth, Appl. Phys. Lett. **66**, 445 (1995).

[21] S. Fukatsu, H. Sunamura, Y. Shiraki, and S. Komiyama, Appl. Phys. Lett. **71**, 258 (1997).

[22] S. Raymond, P. J. Poole, S. Fafard, A. Wojs, P. Hawrylak, S. Charbonneau, D. Leonard, P. M. Petroff, and J. L. Merz, Phys. Rev. B **54**, 11 548 (1996).

[23] S. Sauvage, P. Boucaud, J.-M. Gérard, and V. Thierry-Mieg, Phys. Rev. B **58**, 10 562 (1998).

[24] C. G. Van de Walle and R. M. Martin, Phys. Rev. B **34**, 5621 (1986).

[25] S. K. Chun and K. L. Wang, IEEE Trans. Electron Devices **39**, 2153 (1992).

[26] G. L. G. Sleijpen and H. A. Van der Vorst, SIAM J. Matrix Anal. Appl. **17**, 401 (1996).

[27] R. Häcker and A. Hangleiter, J. Appl. Phys. **75**, 7570 (1994).